Time-resolved optical studies of spin and quasiparticle dynamics in colossal magnetoresistance materials: $La_{0.67}Ca_{0.33}MnO_3$, $La_{0.67}Sr_{0.33}MnO_3$, and Sr_2FeMoO_6

Y. H. Ren,[1,*] M. Ebrahim,[1] H. B. Zhao,[2] G. Lüpke,[2] Z. A. Xu,[3] V. Adyam,[4,†] and Qi Li[4]

[1]*Department of Physics and Astronomy, Hunter College of the City University of New York, New York, New York 10065, USA*

[2]*Department of Applied Science, The College of William and Mary, Williamsburg, Virginia 23187, USA*

[3]*Department of Physics, Zhejiang University, Hangzhou, Zhejiang 310027, China*

[4]*Department of Physics, Pennsylvania State University, University Park, Pennsylvania 16802, USA*

(Received 12 April 2008; revised manuscript received 6 June 2008; published 7 July 2008)

We report on transient reflectivity and magneto-optical Kerr measurements from the colossal magnetoresistance compounds $La_{0.67}Ca_{0.33}MnO_3$ (LCMO), $La_{0.67}Sr_{0.33}MnO_3$ (LSMO), and Sr_2FeMoO_6 (SFMO) as a function of temperature and magnetic field. In LCMO and LSMO, an unusually slow (~ 1 μs) carrier relaxation component is revealed in the transient reflectivity traces. The component disappears as the transition temperature is approached from below. This slow decay process is attributed to spin-lattice relaxation of carriers in localized states and shows a close relationship with the spectral weight near the Fermi surface. The attribution is further supported by our pump-probe magneto-optical Kerr measurements. In addition to the clear observation of magnetic precessions, a long-lived exponentially decaying background reflects the spin-related relaxation of photoexcited electrons. In contrast to manganites, the temperature dependence of transient reflectivity is negligible, although there is a significant change in transient Kerr rotation in SFMO. Our results show that the dynamics of charge, spin, and lattice are strongly correlated with each other in the manganites, but the spin degree of freedom is thermally insulated from the electron and lattice systems.

DOI: 10.1103/PhysRevB.78.014408 PACS number(s): 78.47.−p, 78.20.Ls, 75.47.Gk, 76.70.Hb

I. INTRODUCTION

The mixed-valence perovskite manganites $La_{1-x}Ca_xMnO_3$ attracted a lot of attention recently because of the large drop in electrical resistance in response to the external magnetic field.[1–3] The so-called colossal magnetoresistance (CMR) effect appears near the metal-insulator and the paramagnetic-ferromagnetic transition temperature and reaches a maximum value near $x \approx 0.33$. The close interplay between magnetic and transport properties of $La_{1-x}Ca_xMnO_3$ has long been explained by the ferromagnetic (FM) Mn^{3+}-Mn^{4+} double-exchange interactions accompanied by the Jahn-Teller (JT) distortion of the $Mn^{3+}O_6$, coupling the magnetic and lattice systems at high temperatures.[4–6] The framework of double-exchange interaction qualitatively explains the phenomenology of the CMR effect, but the mechanism alone is insufficient to quantitatively interpret the abnormal transport properties.

Most recently, the role played by an inhomogeneous ground state was outlined by several theoretical and experimental works.[7,8] A prospective picture is the formation of percolative paths for manganese e_g electrons through FM regions. In this context, a temperature-dependent pseudogap has been identified and it drastically suppresses or completely removes the spectral weight (density of states) at the Fermi energy E_F (Ref. 9). The pseudogap is well accounted in models based on electronic phase separation and can be understood based on a picture where ferromagnetic metallic clusters exist in an insulating background.[10] In this scheme, the gradual removal of spectral weight at E_F with temperature is related to the percolative nature of the metal-insulator transition. The region associated with localized carriers (paramagnetic insulating phase) grows while the region with delocalized carriers (ferromagnetic metallic phase) shrinks. As the temperature is raised above T_C, the pseudogap removes nearly all remaining spectral weight at E_F, which is consistent with the insulating behavior of the high-temperature phase. Therefore, the pseudogap appears to be critical for explaining the poor conductivity of both metallic and insulating phases and should be important for explaining the transition between them. So far, although much progress has been made in the characterization of the pseudogap,[11] there are still fundamental questions that need to be answered about the dynamics and mechanisms of the elementary processes related to the pseudogap and their dependence on external perturbations (light, temperature, external magnetic field etc.).

In contrast to the manganites, a new CMR material, double-exchange perovskite Sr_2FeMoO_6 (SFMO), shows a substantial magnetoresistance (MR) at a low applied field even at room temperature[12] and the compound has a ferromagnetic phase transition with the Curie temperature $T_C = 400-450$ K (Ref. 13). From a fundamental point of view, it is even more important to note that crystallographic data do not indicate any JT distortion and the lattice does not appear to play any significant role in the resistivity of this material. The undoped nature of SFMO avoids some sources of disorder and, along with the putative weak electron-phonon coupling, makes this a potentially simpler and cleaner system to understand in detailed theoretical terms, particularly the possible coupling between magnetic and charge degrees of freedom.[14]

The state-of-art time-resolved optical and magneto-optical spectroscopes provide a challenging arena to measure the relaxation dynamics of electronic and spin states in ferromagnets. Dynamical information on the electronic and spin states of the pseudogap can be obtained if charge or spin excitations are introduced via pulsed photoexcitation and the

relaxation processes of the quasiparticles (QPs) are studied on a picosecond time scale. The study of the picosecond magnetization dynamics of manganites was first reported by Zhao *et al.*[15] The authors monitored the optically induced conductance changes in $La_{0.67}Ca_{0.33}MnO_3$ (LCMO) films with 20-ps time resolution and found that long-lived spin excitations are responsible for a resistivity increase in the ferromagnetic phase. So far, several groups have used time-resolved absorption measurements to study the photoinduced response of CMR materials. For example, Kise *et al.* observed an extremely slow relaxation component in their pump-probe magneto-optic Kerr effect (MOKE) spectra. The component has been explained by the isolated spin and electron states in SFMO (Ref. 16). Matsuda *et al.*[17] revealed that the gradual change in 200 ps in the pump-probe absorption spectra reflects the photoinduced demagnetization in $(Nd_{0.5}Sm_{0.5})_{0.6}Sr_{0.4}MnO_3$. Most recently, more detailed studies have been undertaken by Lobad and co-workers and Averitt and co-workers[18–20] They attributed a 100-fs component of the photoinduced absorption in LCMO to electron-lattice thermalization and attributed a slower change in absorption from 20–200 ps to the photoinduced demagnetization driven by the spin-lattice thermalization. Subsequently, Ogasawara *et al.*[21] and McGill *et al.*[22,23] employed the time-resolved MOKE to investigate the magnetization dynamics. Ogasawara *et al.*[21] found that after photoexcitation, the magnetization in $La_{0.6}Sr_{0.4}MnO_3$ decreases with a considerably longer time constant ~ 1 ns, as compared to the one measured by the transient absorption measurements. McGill *et al.*[22,23] recorded the magneto-optic response of LCMO near T_C and observed an even slower Kerr transient, which they attributed to photoinduced spin ordering.

In this paper, we report on time-resolved pump-probe reflectivity and magneto-optical Kerr measurements of photoexcited spin and QP—relaxation dynamics in LCMO, $La_{0.67}Sr_{0.33}MnO_3$ (LSMO), and SFMO as a function of temperature and magnetic field. An unusually slow (~ 1 μs) carrier relaxation component is revealed in the transient reflectivity traces in both LCMO and LSMO. This component disappears as the magnetic transition temperature is approached from below. This slow decay process is attributed to spin relaxation of carriers in isolated states. This is supported by our pump-probe magneto-optical Kerr measurements. A long-lived exponentially decaying background reflects weak magnon scattering of photoexcited electrons, in addition to the observation of spin-wave processions. The behavior of the spin system in SFMO is very different with that of LCMO and LSMO. While the temperature dependence of reflectivity change, $\Delta R/R$ is negligible in SFMO, there is a significant change in its transient MOKE spectra. Our results show that the dynamics of charge, spin, and lattice are strongly correlated with each other in manganites, but electron-spin and electron-lattice interactions are very weak in SFMO.

The outline of this paper is as follows: Section II describes the experimental technique and sample preparation. Section III presents our results and discussion of the long-lived spin-relaxation processes from LCMO and SFMO. Section IV summarizes our results.

II. EXPERIMENTS

The LCMO single crystal was grown by the floating zone method. The LCMO, LSMO, and SFMO films were prepared by pulsed laser deposition (PLD) in an oxygen partial pressure of 10^{-3} Torr from a stoichiometric target on the (100) $SrTiO_3$ or the $NdGaO_3$ (110) substrates. The details of which are reported elsewhere.[24,25] The samples were characterized by electrical resistivity and magnetization measurements. The LCMO single crystal and 400-nm film have Curie temperatures $T_C=225$ and 260 K, respectively. The Curie temperature of the LSMO is ~ 355 K and that of the SFMO is ~ 415 K. The data reported here used a standard transient MOKE and magnetic-field-dependent transient reflectivity setups. The pump-probe experiments were performed in the reflection geometry with various temperatures from 10–450 K. The laser from a Ti-sapphire amplifier system of energy density per pulse ~ 0.1 mJ/cm^2 (pump) and ~ 0.03 mJ/cm^2 (probe), was operating at 800 nm (or at 400 nm) for the CMR samples. The pump pulses induce a transient change of electron and lattice states, which modifies the reflection of the probe pulses that follow behind. We measured the pump-induced change in the field of the reflected probe beam, ΔE_R, also known as the coherent scattered field, as a function of the time delay between the two pulses. To obtain ΔE_R, we determined both the differential reflectivity $\Delta R \propto |E_R + \Delta E_R|^2 - |E_R|^2 \approx 2E_R.\Delta E_R$ (E_R is the reflected probe field when the pump is turned off) and the pump-induced shift of the polarization angle of the reflected probe field, $\Delta\theta$. In particular, $\Delta\theta$ was obtained from differential magneto-optical Kerr measurements in the Voigt geometry using a scheme that gives an output signal proportional to $E_R \times \Delta E_R$. Because scattering by spin-flip excitations is described by an antisymmetric tensor, the signature of a pure-spin magnetic precession is $\Delta E_R \perp E_R$ (or $\Delta R \equiv 0$). This selection rule was found to be strictly obeyed in all our measurements.

III. RESULTS AND DISCUSSION

A. LCMO single crystal and film

Figures 1(a) and 1(b) show the time evolution of ΔR and $\Delta\theta$ from the 400-nm LCMO film at 25 K. The pump wavelength is 800 nm and the probe wavelength is 400 nm. ΔR shows an initially fast biexponential decay with relaxation times $\tau_A \sim 2$ ps and $\tau_B \sim 80$ ps along with weak acoustic phonon oscillations.[26] Also, a very long-lived negative ΔR signal remains sufficiently long, with decay time $\tau_{SL} \sim 1$ μs, that a negative ΔR is clearly observable even after 4 μs (Ref. 27). The negative signal is also present in the time-resolved MOKE spectra. In addition to the clear oscillations due to the precession of magnetization (spin waves), a long-lived exponentially decaying background reflects the spin-related relaxation of photoexcited electrons. In the following, we discuss the temperature and magnetic-field dependence of ΔR at $\Delta t=500$ ps (normalized to its peak value) referred to as $\Delta R'$ (Ref. 28).

Figure 2(a) illustrates the temperature dependence of $\Delta R'$ from the 400-nm LCMO film and LCMO single crystal at

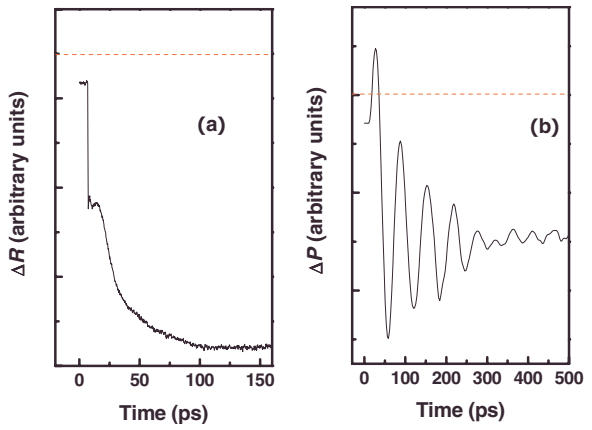

FIG. 1. (Color online) (a) Transient reflectivity ΔR and (b) polarization angle $\Delta\theta$ of the 100-nm LCMO film at 25 K at $\lambda_{pump}=800$ nm/$\lambda_{probe}=400$ nm. The spectrum of transient reflectivity was taken under zero magnetic field and at the spectrum of transient polarization angle was taken under 0.35 T magnetic field applied along the [110] direction. The dashed lines are guides to zero.

800-nm wavelength (both pump and probe). $\Delta R'$ increases with increasing temperature followed by an abrupt drop to a positive value around T_C (the negative component tends to be zero above the magnetic transition temperature). This negative component is present in both the metallic and insulating phase, as observed in the transient optical reflectivity and transmission measurements from LSMO and $Nd_{0.67}Sr_{0.33}MnO_3$ (NSMO) (Ref. 29). However, as shown in Fig. 2(b), there is no evidence of this component in the transient reflectivity change of the paramagnetic phase LSMO, which shows a phase transition from ferromagnetic metal to paramagnetic metal at 355 K. Therefore, we ascribe the long-lived negative component of ΔR to a slow spin-relaxation process of the magnetically ordered phase.

Moreover, we changed the wavelength of pump (and/or probe) from 800 nm to 5.2 μm and realize that $\Delta R'$ is independent of pump and probe wavelength in LCMO. Since the excitation and detection at different wavelengths are related directly to the available density of state near the Fermi level

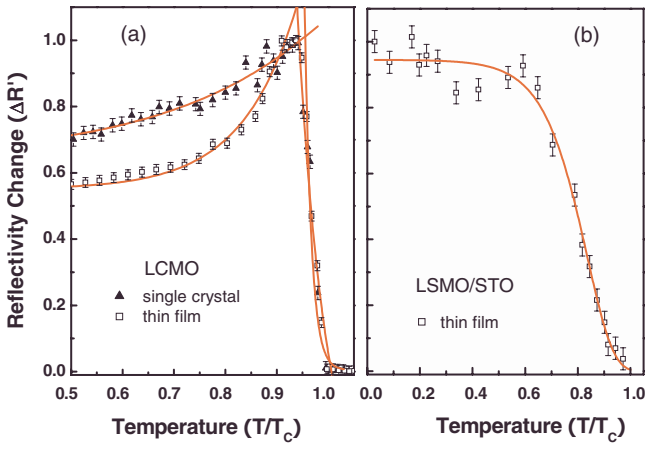

FIG. 2. (Color online) Amplitude of $\Delta R'$ from (a) LCMO film and single crystal and (b) LSMO film as a function of temperature. The solid lines indicate the power-law dependence (Ref. 33).

E_F and the result is, therefore, a strong indication of the presence of the fully spin-aligned pseudogap states.[11,30] The long-lived negative ΔR signal is attributed to the decay of metastable states involving a spin-flip process. The lifetime $\tau_{SL}\sim 1$ μs of these metastable states is comparable with the spin-lattice relaxation time measured by the μSR technique.[31]

The various processes giving rise to the photoinduced reflectivity change in LCMO are depicted in Fig. 3(a). An ultrashort laser pulse first excites electrons via interband transitions. In our experiments, the samples absorbed $\sim 10^{19}$ photons/cm^3 per pulse, comparable to the charge-carrier density ($\sim 10^{20}-10^{21}$ holes/cm^3) in LCMO; hence, one expects significant electron excitation during ultrashort pump pulse illumination. These hot electrons very rapidly release their energy via electron-electron and electron-phonon collisions, $\tau_A\sim 2$ ps, reaching QP states near the Fermi energy (step one). This process generates spin waves (magnons).[32] Spin waves lead to the excitation of metastable states, which decay on μs time scale.[32] Moreover, the QPs can be recombined by interaction with states in the pseudogap τ_B (step two) or relax to metastable states via spin-flip processes (magnons are released) caused by strong electron-lattice coupling (step three). The carriers in the metastable states will relax with a recombination rate $\gamma=1/\tau_{SL}$, while magnons are absorbed (step four). As the pseudogap opens up with increasing temperature and as the spectral weight of states at the Fermi level decreases, the decay rate of excited QPs decreases (step two) and more quasiparticles are scattered into metastable states (step three). This effect leads to the initial rise of $\Delta R'$, which is inversely proportional to the density of states in the pseudogap, i.e., for $T\leq 0.85T_C$ and $\Delta R'\propto(T_C-T)^{-b}$ with $b\approx 0.3-0.5$. With further increasing temperature ($T>0.85T_C$), $\Delta R'$ drops significantly toward zero due to the increase in the density of states and occupation of the down-spin conduction electrons, which introduces magnetic disorder.[33] The fact that the spin-wave oscillations show up in our transient MOKE traces after ~ 2 ps time delay between pump and probe beams [Fig. 1(a)], gives us a direct support of this model. Indeed, the fast spin-lattice interactions (step three) have been discussed thoroughly by Averitt and co-workers and Lobad and co-workers[18–20] in their pump-probe measurements at a low kilohertz repetition rate.

B. LSMO and SFMO films

For comparison, we also did temperature-dependent measurements of $\Delta R'$ in the 400-nm LSMO and the 400-nm SFMO films. In contrast to LCMO, we did not see the increase in $\Delta R'$ near T_C in LSMO, as shown in Fig. 2(b). This is consistent with the fact that the tendency to be in the pseudogap state is much smaller in the large bandwidth manganite (LSMO) than that in the intermediate bandwidth compound (LCMO) (Ref. 34). After QPs are scattered into the metastable states, the magnon relaxation time is mainly determined by the available density of states of the down-spin electrons, which reflects the critical behavior of the magnetic phase transition. As expected, a power-law dependence on

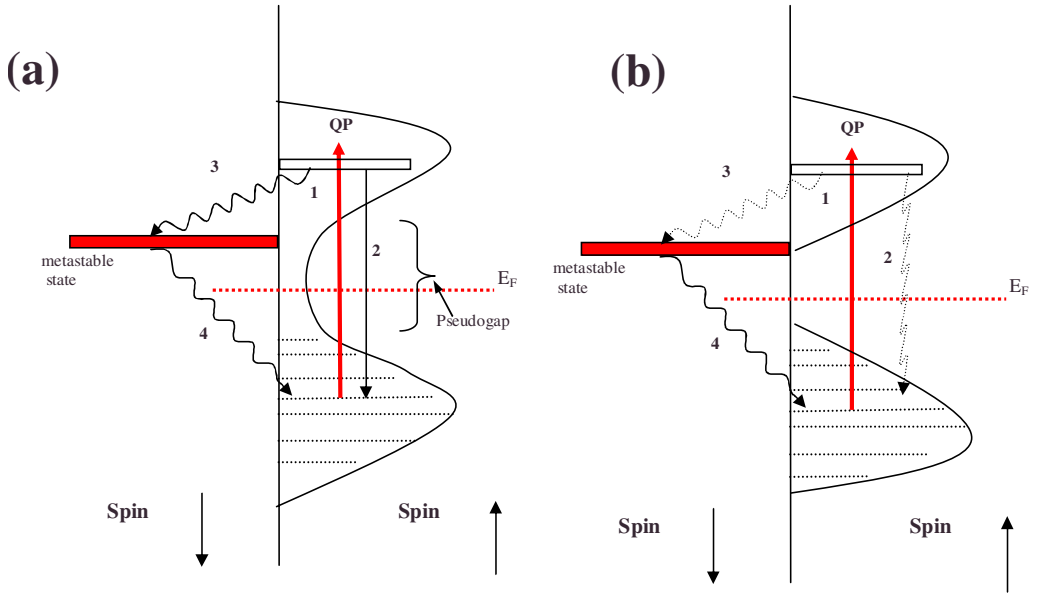

FIG. 3. (Color online) A schematic diagram of carrier excitation/relaxation processes in (a) LCMO and (b) SFMO. For details see text. The dashed lines show weak electron-phonon interactions.

the temperature $\Delta R' \propto [1-(T/T_C)^2]^{\upsilon}$ with $\upsilon \approx 0.15-0.25$ is observed in LSMO. The υ denotes the critical exponent of the magnetic correlation length.

In addition, the various processes described above can be used to correctly explain the temperature dependence of the electron and spin-relaxation processes in the SFMO film. While ΔR is almost temperature independent below T_C in SFMO [Fig. 4(a)], the long-lived component in the transient MOKE spectra shows a strong temperature dependence [Fig. 4(b)]. The results could be understood in terms of the undoped nature of SFMO and its putative weak electron-phonon coupling. First, the slow relaxation process in ΔR reveals an extremely small heat exchange between electrons and lattices and the temperature independence of ΔR below T_C is consistent with a clean gap structure. In the meantime, the slow relaxation of spins reveals that the spin degree of freedom is thermally insulated from the electron and lattice systems. This is due to the half-metal nature of SFMO; the conducting electrons are perfectly spin polarized in the up-spin band and are isolated from the insulating down-spin band.

As shown in Fig. 3(b), initially, during the photoexcitation ($\sim$1 ps), the electron system is heated up and rapidly thermalized due to electron—electron interactions (step one). In this stage, the ΔR shows a sharp decrease. The hot electrons accumulate above the gap ("bottle neck" effect) and form a metastable state ($\sim$2 ps) by the weak electron-phonon interactions. Simultaneously, spin waves are excited due to the strong demagnetization induced by ultrafast pulses in SFMO (step two). The quasiparticles and the magnons relax very slowly back to its initial state by transferring its energy to the lattice system ($\sim$1 ns) (step three) and through weak heat exchange with the electron and lattice systems at quasiequilibrium temperature (step four), respectively. The change of transient Kerr rotation $\Delta\theta$ in SFMO with increasing temperature reflects the gradual loss of spin alignment and, therefore, more magnetic disorder scatterings are expected.

Finally we show magnetic-field dependent measurements of $\Delta R'$ as a function of temperature for LCMO thin film grown on the $NdGaO_3$ (110) substrate (Fig. 5). Magnetic fields are applied in the Faraday geometry, generating an isothermal magnetic entropy change. The results are consistent with our model. The long-lived spin-lattice relaxation dynamics shows strong magnetic-field dependence for B, ranging from 0–3 T. The change in the amplitude of $\Delta R'$ with temperature is due to the increase in T_C with applied magnetic field; this results in an increase in magnetic correlations (spatially and temporally) with enhanced spin alignments. The magnetic correlations are strong enough to overcome thermal fluctuations at the new transition temperature and directly affect the related quasiparticle and spin-

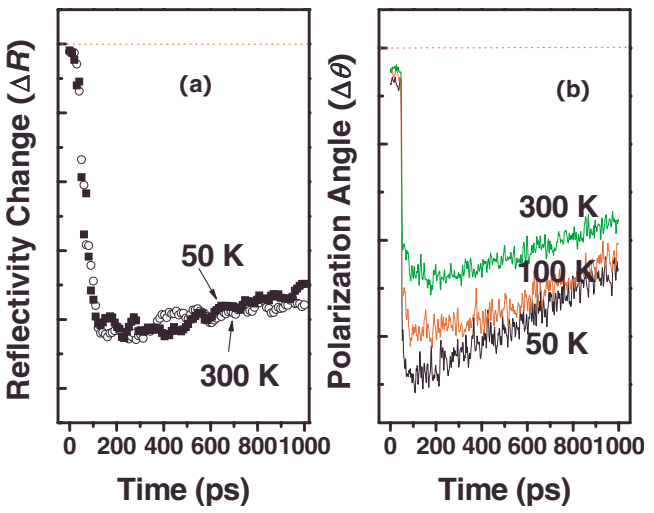

FIG. 4. (Color online) (a) Transient reflectivity ΔR and (b) Kerr rotation angle $\Delta\theta$ of SFMO film at various temperatures at $\lambda_{pump}=400$ nm/$\lambda_{probe}=800$ nm. The dashed lines are guides to zero.

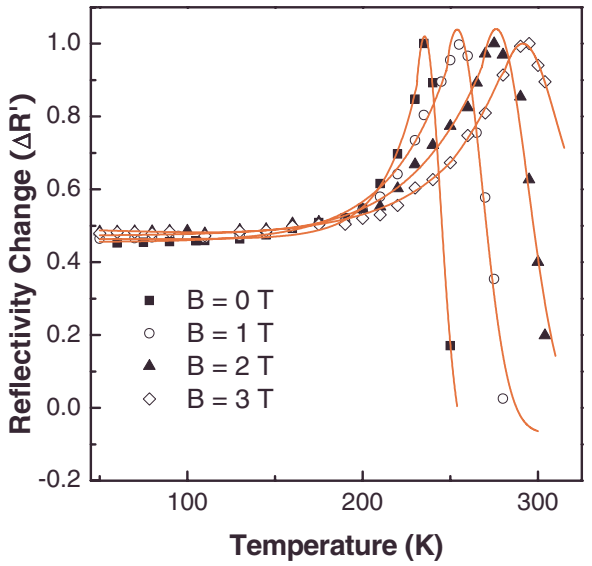

FIG. 5. (Color online) Amplitude of $\Delta R'$ from LCMO film as a function of temperature for applied fields ranging from $B=0$ to 3 T. The solid lines are guides for the eye.

relaxation process. The result clearly excludes the simple thermal origin (heating effect) of the long-lived quasiparticle relaxation component.

IV. CONCLUSION

In summary, we investigated the spin and quasiparticle relaxation dynamics in LCMO, LSMO, and SFMO single crystal and films as a function of temperature and magnetic field by time-resolved pump-probe spectroscopy. The spin and quasiparticle relaxation rates are governed by both the temperature- and magnetic-field dependent pseudogap and magnetization in LCMO but only on magnetization in LSMO. The manganite exhibits metastable (localized) states with lifetime $\tau_{SL} \sim 1$ μs, which decay via strong spin-lattice coupling. Our results show that the coupled dynamics of charge, spin, and lattice are strongly correlated with the distinct gap structures in manganites. In contrast to the manganites, the temperature dependence of transient reflectivity is negligible, although there is a significant change in transient Kerr rotation in SFMO. The slow relaxation of spins reveals that the spin degree of freedom is thermally insulated from the electron and lattice systems in SFMO. This is consistent with the weak electron-phonon coupling and the half-metal nature of the material.

ACKNOWLEDGMENTS

We gratefully acknowledge the support from the Petroleum Research Fund and a PSC-CUNY grant. The research at C.W.M. was supported by a DoE-BES grant.

*yre@hunter.cuny.edu
†Present address: Cryogenic Engineering Centre, Indian Institute of Technology Kharagpur, Kharagpur 721302, India.

[1] R. von Helmolt, J. Wecker, B. Holzapfel, L. Schultz, and K. Samwer, Phys. Rev. Lett. **71**, 2331 (1993).
[2] S. Jin, T. H. Tiefel, M. McCormack, R. A. Fastnacht, R. Ramesh, and L. H. Chen, Science **264**, 413 (1994).
[3] A. Asamitsu, Y. Moritomo, Y. Tomioka, T. Arima, and Y. Tokura, Nature (London) **373**, 407 (1995).
[4] C. Zener, Phys. Rev. **82**, 403 (1951).
[5] P. W. Anderson and H. Hasegawa, Phys. Rev. **100**, 675 (1955).
[6] A. J. Millis, P. B. Littlewood, and B. I. Shraiman, Phys. Rev. Lett. **74**, 5144 (1995).
[7] J. M. De Teresa, M. R. Ibarra, P. A. Algarabel, C. Ritter, C. Marquina, J. Blasco, J. Garcia, A. del Moral, and Z. Arnold, Nature (London) **386**, 256 (1997).
[8] J. Burgy, A. Moreo, and E. Dagotto, Phys. Rev. Lett. **92**, 097202 (2004).
[9] Y.-D. Chuang, A. D. Gromko, D. S. Dessau, T. Kimura, and Y. Tokura, Science **292**, 1509 (2001).
[10] A. Moreo, S. Yunoki, and E. Dagotto, Science **283**, 34 (1999).
[11] T. Saitoh, D. S. Dessau, Y. Moritomo, T. Kimura, Y. Tokura, and N. Hamada, Phys. Rev. B **62**, 1039 (2000).
[12] K.-I. Kobayashi, T. Kimura, H. Sawada, K. Terakura, and Y. Tokura, Nature (London) **395**, 677 (1998).
[13] Y. Tomioka, T. Okuda, Y. Okimoto, R. Kumai, K.-I. Kobayashi, and Y. Tokura, Phys. Rev. B **61**, 422 (2000).
[14] D. D. Sarma,Priya Mahadevan, T. Saha-Dasgupta, Sugata Ray, and Ashwani Kumar, Phys. Rev. Lett. **85**, 2549 (2000).
[15] Y. G. Zhao, J. J. Li, R. Shreekala, H. D. Drew, C. L. Chen, W. L. Cao, C. H. Lee, M. Rajeswari, S. B. Ogale, R. Ramesh, G. Baskaran, and T. Venkatesan, Phys. Rev. Lett. **81**, 1310 (1998).
[16] T. Kise, T. Ogasawara, M. Ashida, Y. Tomioka, Y. Tokura, and M. Kuwata-Gonokami, Phys. Rev. Lett. **85**, 1986 (2000).
[17] K. Matsuda, A. Machida, Y. Moritomo, and A. Nakamura, Phys. Rev. B **58**, R4203 (1998).
[18] A. I. Lobad, R. D. Averitt, C. Kwon, and A. J. Taylor, Appl. Phys. Lett. **77**, 4025 (2000).
[19] A. I. Lobad, R. D. Averitt, and A. J. Taylor, Phys. Rev. B **63**, 060410(R) (2001).
[20] R. D. Averitt, A. I. Lobad, C. Kwon, S. A. Trugman, V. K. Thorsmølle, and A. J. Taylor, Phys. Rev. Lett. **87**, 017401 (2001).
[21] T. Ogasawara, M. Matsubara, Y. Tomioka, M. Kuwata-Gonokami, H. Okamoto, and Y. Tokura, Phys. Rev. B **68**, 180407(R) (2003).
[22] S. A. McGill, R. I. Miller, O. N. Torrens, A. Mamchik, I. Wei Chen, and J. M. Kikkawa, Phys. Rev. Lett. **93**, 047402 (2004).
[23] S. A. McGill, R. I. Miller, O. N. Torrens, A. Mamchik, I. Wei Chen, and J. M. Kikkawa, Phys. Rev. B **71**, 075117 (2005).
[24] H. S. Wang and Qi Li, Appl. Phys. Lett. **73**, 2360 (1998); H. S. Wang, E. Wertz, Y. F. Hu, and Qi Li, J. Appl. Phys. **87**, 7409 (2000).
[25] C. S. Hong, W. S. Kim, E. O. Chi, K. W. Lee, and N. H. Hur, Chem. Mater. **12**, 3509 (2000).
[26] Yuhang Ren, G. Lüpke, Yufeng Hu, Qi Li, C. S. Hong, N. H. Hur, and R. Merlin, Phys. Rev. B **74**, 012405 (2006).

[27] We estimate the ~1 μs relaxation time according to the relative magnitude of the negative transient reflectivity signal before the zero time-delay and at 1 ns position.
[28] Since the magnitude of the transient reflectivity signal changes dramatically with applied external magnetic field and from sample to sample, we normalized the negative signal according to the peak value (when the negative signal reaches its maximum) for comparison. The normalization does not change the physical effect of the negative component.
[29] Y. H. Ren, H. B. Zhao, G. Lüpke, Y. F. Hu and Qi Li, J. Appl. Phys. **91**, 7514 (2002).
[30] J.-H. Park, C. T. Chen, S.-W. Cheong, W. Bao, G. Meigs, V. Chakarian, and Y. U. Idzerda, Phys. Rev. Lett. **76**, 4215 (1996).
[31] R. H. Heffner, J. E. Sonier, D. E. MacLaughlin, G. J. Nieuwenhuys, G. M. Luke, Y. J. Uemura, W. Ratcliff, S.-W. Cheong, and G. Balakrishnan, Phys. Rev. B **63**, 094408 (2001).
[32] J. S. Dodge, A. B. Schumacher, J.-Y. Bigot, D. S. Chemla, N. Ingle, and M. R. Beasley, Phys. Rev. Lett. **83**, 4650 (1999).
[33] The solid curves in Fig. 2(a) are the combination of two power laws, which have been discussed in detail in the model part of the manuscript. The first one is the power law for $T \leq 0.85T_C$. This is mainly due to opening of the pseudogap; which is positive. The second one is the power law for $0.85T_C \leq T < T_C$; this is due to the loss of magnetization in the sample; which is negative.
[34] For a review, see, *Colossal Magnetoresistive Oxides*, edited by Y. Tokura (Gordon and Breach, New York, 2000).